STATISTICAL SHAPE ANALYSIS OF BRAIN STRUCTURES USING SPHERICAL WAVELETS

D Nain[1], *M Styner*[3], *M Niethammer*[4], *J J Levitt*[4], *M E Shenton*[4], *G Gerig*[3], *A Bobick*[1], *A Tannenbaum*[2]

[1] College of Computing, [2] Schools of Electrical & Computer and Biomedical Engineering, Georgia Tech, Atlanta, USA
[3] Deparment of Computer Science and Department of Psychiatry, UNC, Chapel Hill, USA
[4] Department of Psychiatry, VAMC-Brockton, Harvard Medical School, Boston, USA
tannenba@ece.gatech.edu, martin_styner@ieee.org

ABSTRACT

We present a novel method of statistical surface-based morphometry based on the use of non-parametric permutation tests and a spherical wavelet (SWC) shape representation. As an application, we analyze two brain structures, the caudate nucleus and the hippocampus, and compare the results obtained to shape analysis using a sampled point representation. Our results show that the SWC representation indicates new areas of significance preserved under the FDR correction for both the left caudate nucleus and left hippocampus. Additionally, the spherical wavelet representation provides a natural way to interpret the significance results in terms of scale in addition to knowing the spatial location of the regions.

Index Terms— Image shape analysis, Wavelet transforms.

1. INTRODUCTION

The study of brain morphology has emerged as a new field of computational neuroanatomy and can provide great insights into brain pathologies. The aim of our work is to investigate whether there exists morphological differences of selected brain structures between groups of neuropsychiatric patients with neuroanatomic abnormalities and a group of healthy controls. To reach this aim, we compare structures extracted from MRI images of different subjects using statistical tests.

Statistical analysis of brain structures is often based on global features, such as volumetric measurements [1]. However, studies have shown that morphometric analysis of brain structures provides new information which is not available by conventional volumetric measurements [2]. To conduct 3D morphometry, various shape representations have been proposed, ranging from dense sampled 3D Point Distribution Models (PDM) [3, 4] to medial shape descriptions [5, 6, 2, 7] and surface parametrization using expansion into a series of Fourier [8] or spherical harmonic basis functions [9]. Combined, these representations provide new complementary measurement tools to answer clinical research questions.

This work is funded by the National Alliance for Medical Image Computing (NAMIC), NIH Grants U54 EB005149, NIMH R01 MH 50740 and K05 MH 70047, NAC P41 RR-13218 and the VA Merit Award and VA Center Grant in Schizophrenia. The acquisition and segmentation of hippocampal schizophrenia study was funded by the Stanley Foundation.

In this work, we propose to use a spherical wavelet shape representation for statistical shape analysis using permutation tests [10, 11, 12, 13]. The representation is a surface parametrization using expansion into a series of spherical wavelet basis functions, providing a scale space description of shape. When representing shape information, spherical wavelet coefficients have a more intuitive interpretation than Fourier or spherical harmonic coefficients due to the localized nature of spherical wavelet basis functions. Each coefficient describes a portion of the surface and the size of that portion depends on the scale of the coefficient. However coefficients are not as localized as points in a PDM representation, potentially capturing shape characteristics that exist at different spatial locations and different spatial extent, i.e a bending of a portion of the shape. We use this shape representation for statistical shape analysis of two brain structures, the caudate nucleus and hippocampus, and compare the results obtained to shape analysis using a SPHARM-PDM representation.

2. METHODS

2.1. SPHARM-PDM

The input of the proposed shape analysis is a set of binary segmentations of a single brain structure. These segmentations are transformed into a SPHARM-PDM representation using a procedure described in [13]. Here we sketch the major steps of the algorithm. The binary voxel objects provided by expert slice-by-slice segmentations are first preprocessed to fill any interior holes and to smooth boundary voxel noise. The processed binary segmentations are converted to surface meshes, and a spherical parametrization is computed for the surface meshes using an area-preserving, distortion minimizing spherical mapping. The SPHARM description is computed from the mesh and its spherical parametrization. Using the first order ellipsoid from the spherical harmonic coefficients, the spherical parametrizations are aligned to establish correspondence across all surfaces. The SPHARM description is then sampled into a triangulated surface (SPHARM-PDM) via icosahedron subdivision of the spherical parametrization (4 subdivisions). These SPHARM-PDM surfaces are all spatially aligned using rigid Procrustes alignment.

2.2. Spherical Wavelet Shape Representation (SWC)

The spherical wavelet description is computed from the SPHARM-PDM surface. Each surface contains N vertices and has a spherical parametrization. Each shape is expressed in the spherical wavelet basis function by representing it as three signals f^x, f^y and f^z on the discrete sphere, corresponding to the x, y and z coordinates of all vertices. We then expand each signal into a series of spherical wavelet basis functions using the forward spherical wavelet transform [11]:

$$f^x(n) = \sum_j \sum_{k \in Kj} \gamma^x_{j,k} \phi_{j,k}(n) \qquad (1)$$

where $\phi_{j,k}$ is a basis function[1] defined over all vertices indexed by $n \in N$, j denotes the scale (spatial extent) and k the center of the basis function, and $\gamma^x_{j,k}$ is the associated wavelet coefficient. As a result, each shape is represented by a series of spherical wavelet coefficients (SWC). The top row of Figure 1 shows the decreasing spatial support of a single basis function at scales $j = 1, j = 2$ and $j = 3$. Note that the supports of the basis functions overlap across scales but also slightly within a scale. To locate and visualize the influence of all basis functions at a given scale, each point on the sphere is associated to the basis function with the highest value at that point (see middle and bottom rows of Figure 1).

2.3. Shape Analysis

2.3.1. Test Statistic

The difference between a multivariate feature in two groups is computed using a modified Hotelling T^2 two sample metric that is less sensitive to group differences than the standard T^2 metric. Given a group i with n_i samples, we calculate the mean μ_i and covariance Σ_i of a 3D feature. The modified T^2 for two groups is given by:

$$T^2 = (\mu_1 - \mu_2)^T (\Sigma_1 \frac{1}{n_1} + \Sigma_2 \frac{1}{n_2})^{-1} (\mu_1 - \mu_2) \qquad (2)$$

A PDM feature is a point with 3D coordinates. A SWC feature is a basis function $\phi_{j,k}$ with 3D coordinates corresponding to the spherical wavelet coefficients $\gamma^x_{j,k}$, $\gamma^y_{j,k}$ and $\gamma^z_{j,k}$.

2.3.2. Non-parametric permutation tests

We want to test the two groups for differences in the means of the T^2 metric at each feature. Permutation tests are a valid and tractable approach for such an application, as they rely on minimal assumptions and can be applied even when the assumptions of the parametric approach are untenable. Our null hypothesis is that the distribution of the value of each feature is the same for every subject regardless of the group. Given n_1 members of the first group $a_k, k = 1, ..., n_1$ and n_2 members of the second group $b_k, k = 1, ..., n_2$, we can create $M \leq \binom{n_1+n_2}{n_2}$ permutation samples. A value of M from $20,000$ and up should yield results that are negligibly different from using all permutations for a typical experiments of 40 samples in each group [14]. To calculate a P-value for a feature, the real group difference T_0^2 for that feature is compared to the distribution of group differences T_j^2 computed from random permutations of the group labels for that feature. The quantile in the T_j^2 histogram associated with T_0^2 is called the raw P-value. Given a chosen significance value α, the hypothesis that the feature value is the same in both groups is rejected if the P-value for that feature is less than α.

[1] At scale 1, the basis functions are scaling functions.

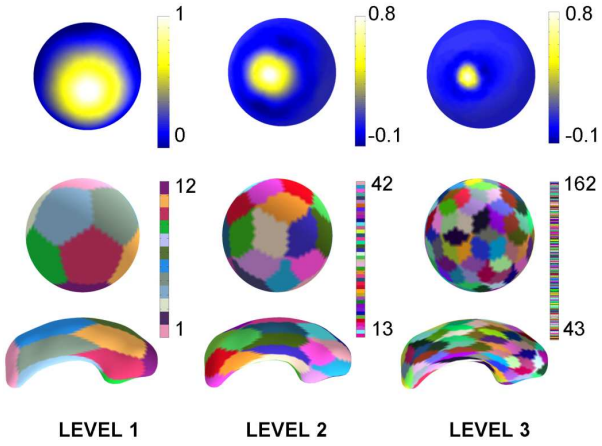

Fig. 1. Visualization of spherical wavelet functions and associated membership regions at three levels (columns). **Top row** : Values of single spherical Wavelet Basis Function shown on the sphere at scales 1 through 3. **Middle and Bottom row**: Membership regions of spherical wavelet basis functions shown on the sphere and on the original surface, coloring is random.

2.3.3. Correction for Multiple Comparisons

Since the shape analysis involves testing from a few to many thousands of hypotheses (one per feature), it is important to control for the multiple testing problem. We use a False Discovery Rate (FDR) estimation, a procedure that controls the expected proportion of false positives among those tests for which a local significance has been detected [13]. FDR allows an expected proportion (usually 5%) of the FDR-corrected significance values to be falsely positive.

2.4. Significance Map Visualization

For PDM features, we visualize both the raw and FDR corrected P-values as significance color maps on the surface of the mean shape of the structure under study. The color at each point is the P-value. For SWC features, we would also like to build such a significance map. If a feature (basis function) is found significant, we color all points that are in the support of that basis function at that scale with the corresponding P-value. If more than one basis function is found significant and the support of the basis functions overlap, we assign the overlapping region to the function with higher value, and color the region with the P-value of that basis function.

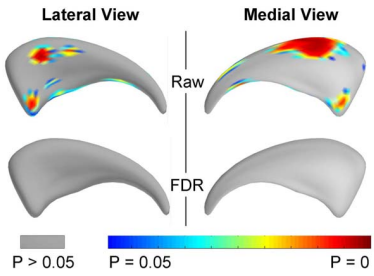

Fig. 2. Left Caudate Shape Analysis Results - Significance maps for the PDM features. This figure is best seen in color.

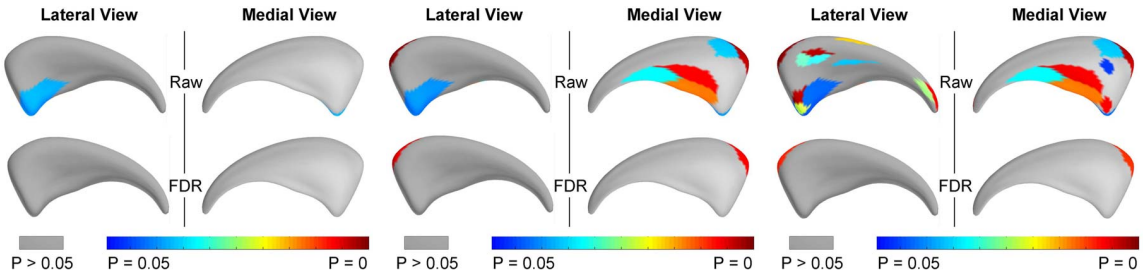

(a) **SWC SCALE 1** (b) **SWC SCALES 1-2** (c) **SWC SCALES 1-3**

Fig. 3. Left Caudate Shape Analysis Results - Significance maps for the SWC features. This figure is best seen in color.

3. RESULTS

We applied our shape analysis framework using both the PDM features and SWC features to two studies[2]. The first is a schizo-typal personality disorder (SPD) study on the caudate brain structure in female adult patients [15]. 32 SPD subjects and 29 healthy control subjects were analyzed. The second is a schizophrenia study on the hippocampus brain structure in male adult schizophrenia [7]. 56 schizophrenia subjects and 26 healthy control subjects were analyzed. The subjects in both studies have same handedness and the structures were corrected for difference in head size.

For both structures, we analyzed the right and left hemisphere separately. We present results on left structures for brevity. For SWC features, the shape analysis is conducted at various cumulative scales: all features associated to basis functions up to a given scale are tested for difference among the groups. For all structures we present results up to scale 3 since no new features were discovered at subsequent scales[3].

3.1. Left Caudate Nucleus

The result for PDM is shown in Figure 2. The raw significance map displays an overly optimistic estimate of significance in the superior body and anterior head region. The FDR-corrected map is a more pessimistic estimate and does not show any significance. The result for SWC are shown in Figures 3(a)-3(c). For the raw map (top rows), scale 1 displays significance at the anterior inferior head region. At cumulative scales 1-2 and 1-3, the raw map displays additional significance in the anterior superior head region, as well as superior body and posterior tail. Overall, the SWC raw map at scales 1-3 displays similar significant areas than the raw PDM map. However, unlike the PDM FDR map, the SWC FDR map displays significant area in the anterior superior region (raw P-value 5e-5, FDR P-value 0.0085).

3.2. Left Hippocampus

The result for PDM is shown in Figure 4. The raw significance map displays significance both in the superior-anterior and inferior-posterior regions. The FDR-corrected map is a more pessimistic estimate and does not show any significance. The result for SWC are shown in Figures 5(a)-5(c). At scale 1, the raw significance map displays significance in the superior and inferior region, indicating that these differences occur already at a coarse scale. At scales 1-2 and 1-3, additional smaller regions of significance appear in the superior-anterior and inferior-posterior, similar to the PDM regions, indicating those group difference are at a fine scale (small spatial support). At scale 1, the FDR map preserves the significance in most regions, and at scale 1-3 a small region in the medial side is preserved (raw P-value 0.0001, FDR P-value 0.016). The FDR correction is more severe at higher scales due to the increasing number of tests, and only preserves the regions with high significance.

Overall, we see that the results for SWC nicely complement the PDM results by showing similar significance regions and providing additional significance regions, even with FDR correction. Additionally, it provides information about the scale of the group difference.

[2]GE 1.5 Tesla MR system using a 3D IR Prepped SPGR acquisition protocol with a 256x256x124 image matrix at 0.9375x0.9375x1.5mm resolution.

[3]Scripts to conduct such analysis are available open-source at www.na-mic.org/Wiki/index.php/Algorithm:GATech:Multiscale_Shape_Analysis

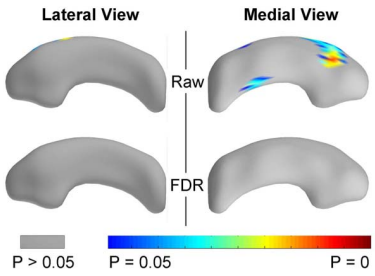

Fig. 4. Left Hippocampus Shape Analysis Results - Significance maps for the PDM features. This figure is best seen in color.

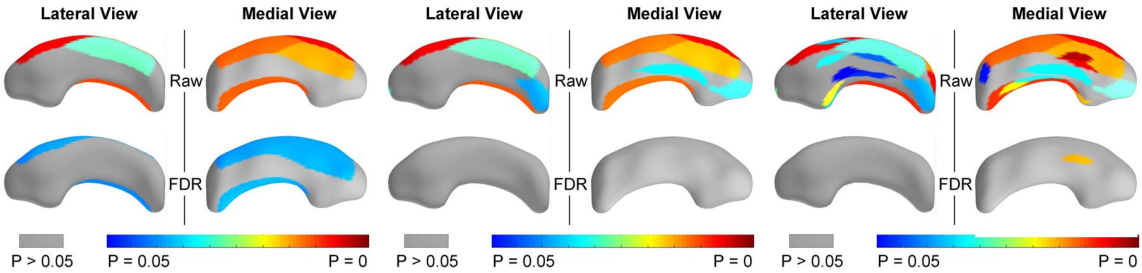

(a) **SWC SCALE 1** (b) **SWC SCALES 1-2** (c) **SWC SCALES 1-3**

Fig. 5. Left Hippocampus Shape Analysis Results - Significance maps for the SWC features. This figure is best seen in color.

4. CONCLUSION

We have presented a novel method for statistical analysis of morphological differences of brain structures based on a spherical wavelet (SWC) representation and compared it to a similar analysis with a PDM representation. The scale-space decomposition of the SWC provides shape features that describe group differences at a variety of scales and spatial locations, providing additional information in addition to local features such as PDM. Indeed the results show that the SWC representation nicely complements the PDM results by indicating new areas of significance preserved under the FDR correction for both the left caudate nucleus and left hippocampus. Further studies providing correction for age and medication will be needed to draw clinical conclusions.

5. REFERENCES

[1] J.J Levitt, R.W. McCarley RW, C.C. Dickey, M.M. Voglmaier, M.A. Niznikiewicz, L.J. Seidman, Y. Hirayasu, A.A. Ciszewski, R. Kikinis, F.A. Jolesz, and M.E. Shenton, "MRI study of caudate nucleus volume and its cognitive correlates in neuroleptic-naive patients with schizotypal personality disorder," *Am J. Psychiatry*, vol. 159, no. 7, pp. 1190–97, 2002.

[2] G Gerig, M Styner, M E. Shenton, and J A. Lieberman, "Shape versus size: Improved understanding of the morphology of brain structures," in *MICCAI*, 2001, LNCS 2208, pp. 24–32.

[3] T.F. Cootes, C.J. Taylor, D.H. Cooper, and J. Graham, "Active shape models - their training and application," *Comp Vis and Image Understanding*, vol. 61, no. 1, pp. 38–59, 1995.

[4] M Styner, JA Lieberman, RK McClure, DR Weingberger, DW Jones, and G Gerig, "Morphometric analysis of lateral ventricles in schizophrenia and healthy controls regarding genetic and disease- specific factors," *Proceedings of the National Academy of Science*, vol. 102, no. 12, pp. 4872–4877, March 2005.

[5] P. Golland, W.E.L. Grimson, and R. Kikinis, "Statistical shape analysis using fixed topology skeletons: Corpus callosum study," in *IPMI*, 1999, LNCS 1613, pp. 382–387.

[6] S. Pizer, D. Fritsch, P. Yushkevich, V. Johnson, and E. Chaney, "Segmentation, registration, and measurement of shape variation via image object shape," *IEEE Trans. Med. Imaging*, vol. 18, pp. 851–865, October 1999.

[7] M. Styner, J. Lieberman, D. Pantazis, and G. Gerig, "Boundary and medial shape analysis of the hippocampus in schizophrenia," *Medical Image Analysis*, vol. 8, no. 3, pp. 197–203, 2004.

[8] L.H. Staib and J.S. Duncan, "Deformable fourier models for surface finding in 3d images," in *Proc. 2nd. Conf. on Vis. in Biomed. Computing*, 1992, vol. 1808, pp. 90–104.

[9] C. Brechbühler, G. Gerig, and O. Kübler, "Parametrization of closed surfaces for 3-d shape description," *Comp Vis and Image Understanding*, vol. 61, no. 2, pp. 154–170, March 1995.

[10] Peter Schröder and Wim Sweldens, "Spherical wavelets: Efficiently representing functions on the sphere," *Computer Graphics Proceedings (SIGGRAPH 95)*, pp. 161–172, 1995.

[11] D. Nain, S. Haker, A. Bobick, and A. Tannenbaum, "Multiscale 3d shape analysis using spherical wavelets," in *MICCAI*, 2005, LNCS 3750, pp. 459–467.

[12] P. Yu, F. Segonne, X. Han, and B. Fischl, "Shape analysis of neuroanatomical structures based on spherical wavelets," in *Human Brain Mapping (HBM)*, 2005.

[13] M Styner, I Oguz, S Xu, C Brechbuhler, D Pantazis, J Levitt, M Shenton, and G Gerig, "Framework for the statistical shape analysis of brain structures using spharm-pdm," Open Science Workshop at MICCAI 2006.

[14] E.S. Edgington, Ed., *Randomization Tests*, Acad Press, 1995.

[15] Koo MS, Levitt JJ, McCarley RW, Seidman LJ, Dickey CC, Niznikiewicz MA, Voglmaier MM, Zamani P andLong KL, Kim SS, and Shenton ME., "Reduction of caudate volume in neuroleptic-naive female subjects with schizotypal personality disorder," *Biol Psychiatry 2006*, vol. 1, no. 60, pp. 40–48.